water

MDPI

Article

Ecological Compensation Mechanism in a Trans-Provincial River Basin: A Hydrological/Water-Quality Modeling-Based Analysis

Wenhua Wan [1], Hang Zheng [1,*], Yueyi Liu [1], Jianshi Zhao [2], Yingqi Fan [1] and Hongbo Fan [1]

[1] School of Environment and Civil Engineering, Dongguan University of Technology, Dongguan 523808, China
[2] State Key Laboratory of Hydro-Science and Engineering, Department of Hydraulic Engineering, Tsinghua University, Beijing 100084, China
* Correspondence: zhenghang00@163.com

Abstract: Ecological compensation is an important economic means of water pollution control and quality management, especially for trans-regional rivers with unbalanced economic and social development between upstream and downstream. The Tangbai River Basin (TRB), a watershed crossing Henan province and Hubei province, China, forms one of the nation's most productive agricultural regions. The TRB has been exposed to high doses of fertilizers for a long time. This study simulates hydrologic and nutrient cycling in the TRB using Soil and Water Assessment Tool (SWAT) with limited data available. The results indicate that dryland fields, which constitute 62% of the basin area, produce 80% of total nitrogen (TN) and 85% of total phosphorus (TP) yields of the whole river basin. The water quality of river sections at the provincial boundary shows that only 29% of the time from 2000 to 2019 met the Class III standard regarding TN and TP concentrations, and the concentrations in the spring flood season are approximately three times the mean in the non-flood season. The Grain for Green ecological restoration measure in Henan province shows that restoration of non-flat drylands can reduce nutrient loads at trans-provincial sections by 3.5 times compared to that of slope-independent drylands; however, the water quality compliance rate remains similar. The value of ecological compensation can also vary widely depending on different quantitative criteria. The SWAT-based pollutant quantification method adopted in this study could have implications for ecological compensation in trans-regional rivers.

Keywords: ecological compensation; trans-regional river; non-point-source pollution; grain for green; SWAT

Citation: Wan, W.; Zheng, H.; Liu, Y.; Zhao, J.; Fan, Y.; Fan, H. Ecological Compensation Mechanism in a Trans-Provincial River Basin: A Hydrological/Water-Quality Modeling-Based Analysis. *Water* **2022**, *14*, 2542. https://doi.org/10.3390/w14162542

Academic Editors: Dengfeng Liu, Hui Liu and Xianmeng Meng

Received: 4 July 2022
Accepted: 15 August 2022
Published: 18 August 2022

1. Introduction

Water pollution control and sustainable development of international river basins have been a major challenge in the current ecological research. Yet, due to the difficulty of data acquisition, reluctant cooperation across boundaries, and the absence of exchange mechanisms [1,2], there are few successful cases. Also arising from unbalanced development along rivers, the trans-provincial river management is a regional form of trans-boundary problem. However, provinces (or states) are more willing to cooperate in controlling pollution than countries given sovereignty and territorial integrity. Successful cases include the Murray–Darling Basin in Australia [3], Delaware River in the United States [4], and Xin'an River in China [5]. Therefore, the management of trans-provincial river basins in water ecology can provide valuable information for solving trans-boundary ecological issues.

Ecological compensation (hereinafter "eco-compensation") has long been considered an effective economic instrument for controlling water pollution in trans-regional basins

[6]. Eco-compensation, also known as "payment for environmental services", was proposed in the late 1990s for watershed management to address the environmental problems caused by the Industrial Revolution [7]. At present, eco-compensation has captured increasing attention nationwide and is seen as a promising complementary method to alleviate the identified contradiction among stakeholders [8]. The form of eco-compensation measures varies by country. In China, the central government has launched a series of explorations and research projects for eco-compensation since 1999. One typical scheme is the national-scale Grain for Green Program, which compensates rural households for converting sloping croplands to forests or grasslands to reduce soil erosion [9,10]. At the local administrative level, the first trans-provincial eco-compensation pilot scheme is the Xin'an River scheme, launched in 2011. This is an eco-compensation agreement between Anhui and Zhejiang provinces, targeting pollution control from the upper regions in Huangshan city, Anhui, and thereby maintaining high water quality in the lower reaches, Qiandao Lake in Hangzhou city, Zhejiang [11]. The list of other pilot eco-compensation schemes in China is found in Wang et al. [12]. These studies are crucial in clarifying the implications of watershed eco-compensation and establishing typical methods and standards. How to reasonably account for compensation and what measures should be taken to effectively protect trans-regional watersheds from water pollution depend largely on the accurate mapping of compensation stakeholders [13]. A solution generally lies in addressing the four questions below. First, what are the major water pollutants and where do they come from? Second, how do pollutants change throughout their journey from upstream to downstream, and are they accumulating or separating? Third, what actions could be taken to reduce the load across regional boundaries? Last, but not least, what is the cost of pollution control and how should it be compensated?

Despite a number of studies on these questions, there is still a lack of systematic quantitative analysis on how eco-compensation responds to the dynamic change in pollutants. Previous scholars from different disciplines have investigated the effectiveness of eco-compensation and measures of reducing water pollution from different perspectives. For research on eco-compensation, current studies primarily focus on policy analysis involving game theory [6] and water-related regulations [11]. However, such methods are mostly static and disregard the responses to hydrology and water quality and, thus, cannot adequately address non-point-source pollution.

In pollution control, the wide range of substances that may pollute water bodies leads to a variety of options for reducing pollution [14,15]. In China, more than 2600 lakes, including the nation's largest freshwater lake, Poyang Lake, have been subjected to high loads of nitrogen (N) and phosphorus (P) [16,17]. Agricultural operations, including crop fertilization and livestock farming, are one of the major sources of N and P pollution to surface water. For example, Boesch et al. [18] and Reckhow et al. [14] found that high nutrient leaching from farmland into the US Chesapeake Bay is the foremost water quality concern for the waterway, and thus nearby agricultural land needs to implement the best management practices. Successful tracking of pollution control strategies relies upon the careful modeling of non-point nutrient fluxes, and distributed process-based models are then introduced [19–21]. These models include, but are not limited to, Soil and Water Assessment Tool (SWAT) [22], Integrated Valuation of Environmental Services and Tradeoffs (InVEST) [23], and Annualized AGricultural Non-point Source (AnnAGNPS) [24]. Among these, SWAT is arguably the most widely used model, especially at the watershed scale [25,26]. In summary, the above scattered studies reveal a fragmented and insufficient link between non-point-source simulation and eco-compensation, thereby failing to support effective policy formulation.

To help decision-makers understand trans-regional non-point-source pollution issues from both environmental and economic perspectives, this study utilized the SWAT hydrological/water-quality model to simulate nitrogen/phosphorus cycling and their responses to eco-compensation strategies for an agricultural watershed, the Tangbai River Basin (TRB). As the TRB receives the most runoff in Henan province and joins the Han

River, the longest tributary of the Yangtze River, in Hubei province, it is a representative trans-provincial river basin. A watershed eco-compensation mechanism is selected as a water pollution control measure to provide a reference for trans-boundary water quality management.

2. Data and Methodology

2.1. Study Area

The Tangbai River Basin (TRB, 31°38′–33°43′ N, 111°34′–113°40′ E, 24,190 km², Figure 1) is a subbasin of the Han River Basin, which is the source of the central route of the South-to-North Water Transfer Project. The Tangbai River is formed by the convergence of two tributaries, the Tang River and the Bai River, flowing through Henan province and Hubei province, China (Figure 1b). The average flow rate at the basin outlet is 323 m³/s (1980–2012 time series). The two tributaries both originate from Nanyang city, the south-western part of Henan province, and then flow into Xiangyang city of Hubei province and finally form the Tangbai River, which later joins the Han River.

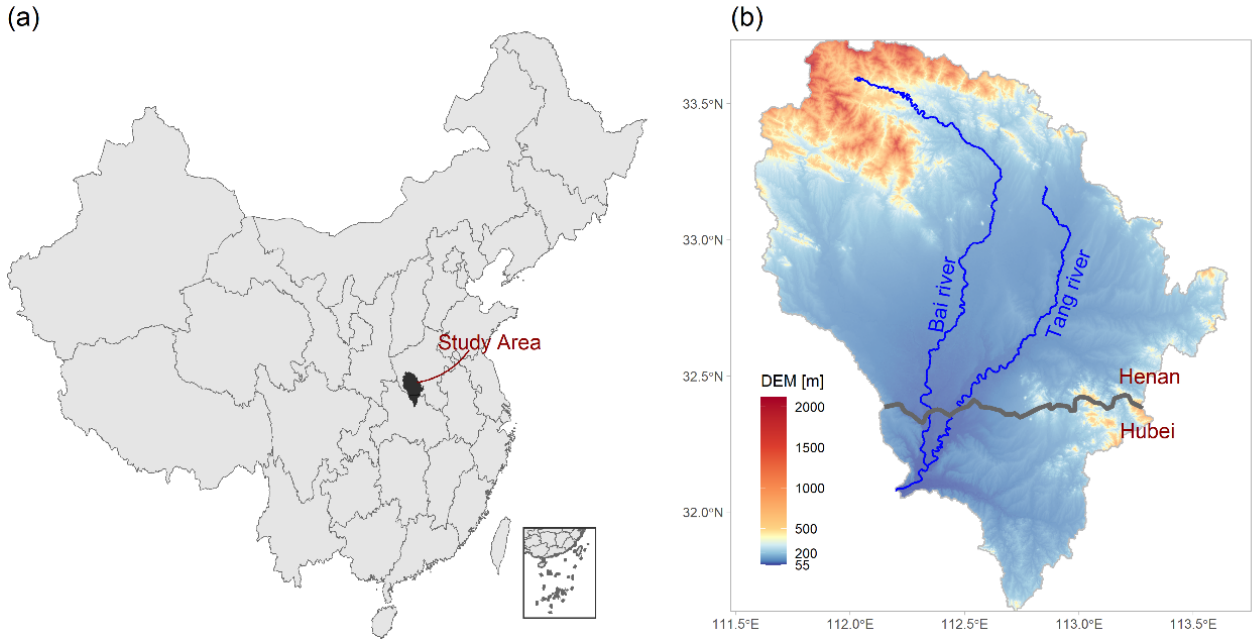

Figure 1. Geographic location (**a**) and 90 m digital elevation map (DEM, **b**) of the Tangbai River Basin, a shared river basin of Henan province and Hubei province. The curved path in (**b**) is the provincial boundary, and the blue lines are the two major tributaries constituting the Tangbai River.

The TRB is characterized by a dense population. Around 90,000 people live in the middle and upper reaches of the watershed, which is the famous Nanyang Basin, the nation's most productive agricultural regions. The excess use of fertilizers, traditional inadequate farming techniques, and dramatic growth of industrial and decreasing runoff during the 1990s due to climate change have led to serious pollution and environmental degradation of the Tangbai River [27]. In recent years, the surface water quality has improved to a common Class IV status due to the long-term regional cooperative actions and joint management between Nanyang (in Henan province) and Xiangyang (in Hubei province) [28]. However, such pollution control mainly focuses on point-source pollution from manufacturing and runoff pollution from urban areas [29]. The agricultural non-point-source pollution in the rural areas of Nanyang city is still prominent. The rainfall- and snowmelt-runoff processes affect the transfer of non-point-source pollution, and thereby disturb the availability of water resources between Nanyang and Xiangyang. As a typical trans-

provincial watershed, managing non-point-source pollution in TRB remains complicated and difficult.

2.2. SWAT Model and Inputs

The SWAT model is a typical semi-distributed, physically-based hydrological model. It splits the watershed into subbasins connected by a stream network and further delineates each subbasin into hydrologic response units (HRUs), which comprise unique combinations of land use, soil type, and slope. The HRU aggregates water and nutrient fluxes to the subbasin level, and they are then routed through the stream network to the watershed outlet. Therefore, the major model inputs consist of topography, land-cover type, soil property, climate data, and land management practices. The resolution and sources of all data inputs in this study are listed in Table 1.

Table 1. Input and validation datasets, sources, and main attributes.

Data Type	Resolution	Year	Data Source
1. Digital elevation model	90 m	2006	SRTM Digital Elevation Database v4. 1 (https://bigdata.cgiar.org/srtm-90m-digital-elevation-database/, accessed on 1 February 2021)
2. Land use land cover	1 km	2000, 2005, 2010, 2015	Resource and Environment Science and Data Center (https://www.resdc.cn/, accessed on 1 February 2021)
3. Soil map	1 km	1995	Resource and Environment Data Cloud Platform (https://www.resdc.cn/, accessed on 1 March 2021); China Soil Science Database (http://vdb3.soil.csdb.cn/, accessed on 1 May 2021); SPAW software (https://hrsl.ba.ars.usda.gov/SPAW/, accessed on 1 May 2021)
4. Climate observation (i.e., station location, precipitation, temperature, solar, relative humidity, solar radiation, wind speed)	daily	1960–2019	National Meteorological Information Centre (http://data.cma.cn/, accessed on 1 February 2021); Angstrom-Prescott radiation model
5. Crop management (i.e., land cover, type, and mode)	date	2019	Field survey
6. Fertilization application (i.e., type, date, and quantity)	date	2005	Field survey; literature review [1]
7. Livestock manure production	daily	2011	Literature review
8. Streamflow data (i.e., station location, flow rate)	monthly	1997–2001; 2007–2012	Changjiang Water Resources Commission of the Ministry of Water Resources
9. Water quality data (i.e., monitoring location, and total nitrogen and phosphorus)	date	2000–2019	Literature review; Monthly Report on Water Quality of Han River (http://sthjj.xiangyang.gov.cn/hjxx/tjsj/hjszyb/, accessed on 1 May 2021); Xiangyang Municipal Ecological Environment Bureau

Note: [1] Namely, statistical analyses of the results of a government-led survey conducted in 2005 on the agricultural pollution along the central route of the South-to-North Water Transfer Project.

In this study, we used the ArcSWAT interface (version 2012) for ArcGIS. The simulation was performed with a monthly time step from 1998–2019, in which the first two years were excluded from the analysis as they were used as the warmup period.

2.2.1. Datasets for SWAT Model Building

A digital elevation model (DEM, 90 m × 90 m, Figure 1b) was used to delineate the watershed. We obtained a DEM from the SRTM 90 m Digital Elevation Database (https://bigdata.cgiar.org/, accessed on 1 February 2021) and clipped it into the area that covers the whole TRB. Note that additional subbasin outlets were manually defined at the locations with hydrological gauging stations (Figure 2d) in addition to the autogenerated subbasins, allowing us to compare the simulated results with observations at any location of interest.

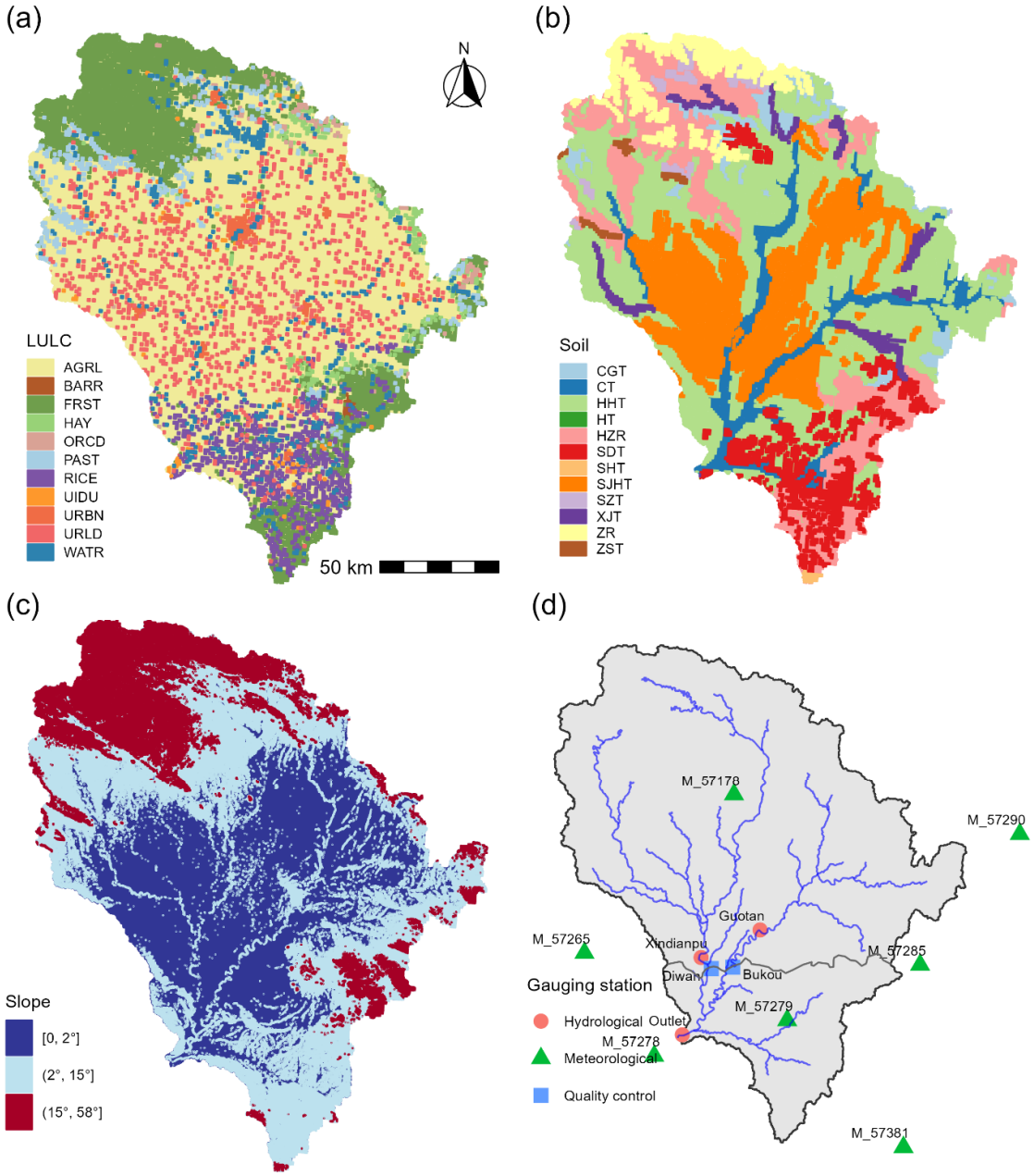

Figure 2. The spatial distribution of the land-use/land-cover (LULC) classes in 2015 (**a**), soil types (**b**), slope classes (**c**), and (**d**) gauging stations in the SWAT-generated stream network, distinguishing meteorological stations used for building SWAT (triangle), hydrological stations used for model validation (circle), and water quality monitoring sections at the provincial boundary (square). Abbreviations of land-cover classes and soil types are found in the main text.

Approximately 66% of the study area is in agricultural use (AGRL and RICE). The remaining area is covered by forest (FRST), grassland (PAST and HAY), residential zones (URLD and URBN), and others. As the area under cultivation changed only slightly from 2000 to 2015, with the dryland (AGRL) decreasing from 62.4% to 61.6% and the paddy field (RICE) increasing from 4.4% to 4.5%, we therefore categorized land-use/land-cover classes based on the conditions in 2015 (Figure 2a). A total of 18.4% of the land-cover area was considered to be mixed forest (FRST), and 6.8% was considered to be low density residential zones. Both the land-cover map and soil map hold a resolution of 1 km × 1 km. The soil characteristics for preparing the user-defined soil database include soil component parameters (e.g., soil name, hydrological soil group, and number of soil layers) and soil layer parameters (e.g., soil depth, salinity, organic matter content, and particle size distribution). All characteristics, except for the soil name, were extracted from the China Soil Science Database (http://vdb3.soil.csdb.cn/, accessed on 1 May 2021) for central China, with some further calculations using SPAW software (Table 1). The most dominant soil types are yellow-cinnamon soil (HHT, 37.4%), shajiang black soil (SJHT, 19.3%), and yellow-brown earth (HZR, 15.2%). The remaining soil types include skeletal soil (CGT), fluvo-aquic soil (CT), cinnamon soil (HT), paddy soil (SDT), lime soil (SHT), litho soil (SZT), alluvial soil (XJT), brown earth (ZR), and purplish soil (ZST). Considering the large span of slope in TRB (i.e., 0–163%, 0–58°), it is necessary to categorize the slope into separate classes. Referring to the soil erosion condition on the steepness of cultivated fields [30], we divided the whole TRB into three slope classes: 0–3.5% (i.e., 0–2°, flat land with no soil erosion), 3.5%–26.8% (i.e., 2–15°, terraced land with a low soil erosion rate), and 26.8–9999% (i.e., 15–58°, sloping land with a high erosion rate) (Figure 2c).

The meteorological observations used were obtained from the National Meteorological Information Centre (Table 1) and consist of rainfall, temperature, relative humidity, solar radiation, and wind speed from seven stations (Figure 2d). Solar radiation was calculated based on sunshine observations using the Angstrom–Prescott equation. Stations outside the watershed were also included for more accurate spatial interpolation of climate data, particularly near the border.

2.2.2. Management Practices for the SWAT Model

To obtain a relatively accurate estimation of crop yields and nutrient transformations in the TRB, we investigated crop rotation, fertilization, and livestock breeding practices based on field surveys and literature review (Tables 1 and 2). Specifically, these management activities were established for three types of land cover: AGRL, RICE, and URLD. As listed in Table 2, the main crops in the AGRL field are rainfed grains (winter wheat, summer corn) with rotation [31], while the RICE field is used for growing rice [32]. The nitrogen fertilizer applied was urea, and the phosphorus fertilizer was phosphorus pentoxide. The amount and fertilization period were set following Lan [33] and local crop guidance [34]. The irrigation schedule was set as default. As livestock and poultry breeding is mainly concentrated in Nanyang city and much less in Xiangyang city, we assumed that in the model all animal breeding occurs in Nanyang in low-density residential zones (URLD). The total amount of fresh manure discharge F_{manure} is then estimated based on the statistics of animal breeding [35], with

$$F_{manure} = \mu \sum_i n_i X_i \, \mathrm{Area}_{TRB} / \mathrm{Area}_{URLD} \quad (1)$$

where μ is the fraction of livestock and poultry manure, which is set to 0.9 according to Cai [32], n_i is the number of the ith specific livestock or poultry breeding, and X_i is manure produced per unit area (kg/ha·d); Area_{TRB} and Area_{URLD} are the area of TRB (ha) and area covered by URLD in TRB (ha).

Table 2. Settings on non-point-source pollution from planting in terms of crop cycle and management practices, and livestock breeding in terms of manure discharge in rural areas based on land cover in 2015.

LULC	Crop	Cycle	Fertilization	Urea Applied (kg/ha)	P_2O_5 [2] Applied (kg/ha)	Fertilizer on Surface
AGRL [1]	Winter wheat	15 October–15 June	15 October	100.38	102.60	0.2
			1 April	43.02	-	0.2
	Summer corn	1 July–15 September	1 August	191.25	59.25	0.2
RICE [1]	Rice	15 April–1 October	1 May	82.80	114.75	0.5
			1 July	49.68	-	0.5
			1 August	33.12	-	0.5
LULC	**Livestock**	**Duration (days)**	**Application frequency**	**Manure [3] applied (kg/ha)**		**Heat Unit**
URLD	Swine/beef/broiler	365	1 (daily)	6.38		0

Note: [1] The auto-fertilization based on heat unit in AGRL and RICE fields were removed. [2] P_2O_5 is a self-defined P fertilizer, in which the fraction of mineral P is 0.43. [3] Compound manure is a self-defined compound manure, in which nutrient fractions are proportional to that of the fresh manure produced by different livestock/poultry species.

Three variants of fertilization were considered depending on land-cover classes: (1) for crop fields (i.e., AGRL and RICE) listed in Table 2, fertilizer was applied according to the calendar; (2) for animal breeding areas (i.e., URLD), compound fresh manure was applied once every day in the form of continuous fertilization; (3) for the remaining land-cover types, an auto-fertilization mode was adopted based on plant nitrogen stress.

Data used for validation include recorded time series of streamflow and water quality. The monthly streamflow was available at three stations on two tributaries: Guotan station (32°32′ N, 112°36′ E) on the Tang River, Xindianpu station (32°25′ N, 112°18′ E) on the Bai River, and at the watershed outlet (32°5′ N, 112°12′ E) (Figure 2d). The streamflow time series span from 1997 to 2012, with 2001–2006 missing. Regarding water quality data, we did not find any long-term observations. We therefore decided to use data from articles and online reports, e.g., [28,36,37], in which nutrients (N and P) are presented in concentration. Data on TN and TP concentrations were collected on different dates, at eight different sites (Figure 3d), including the two river sections at the provincial boundary (Bukou section on the Tang River and Diwan section on the Bai River, Figure 2d).

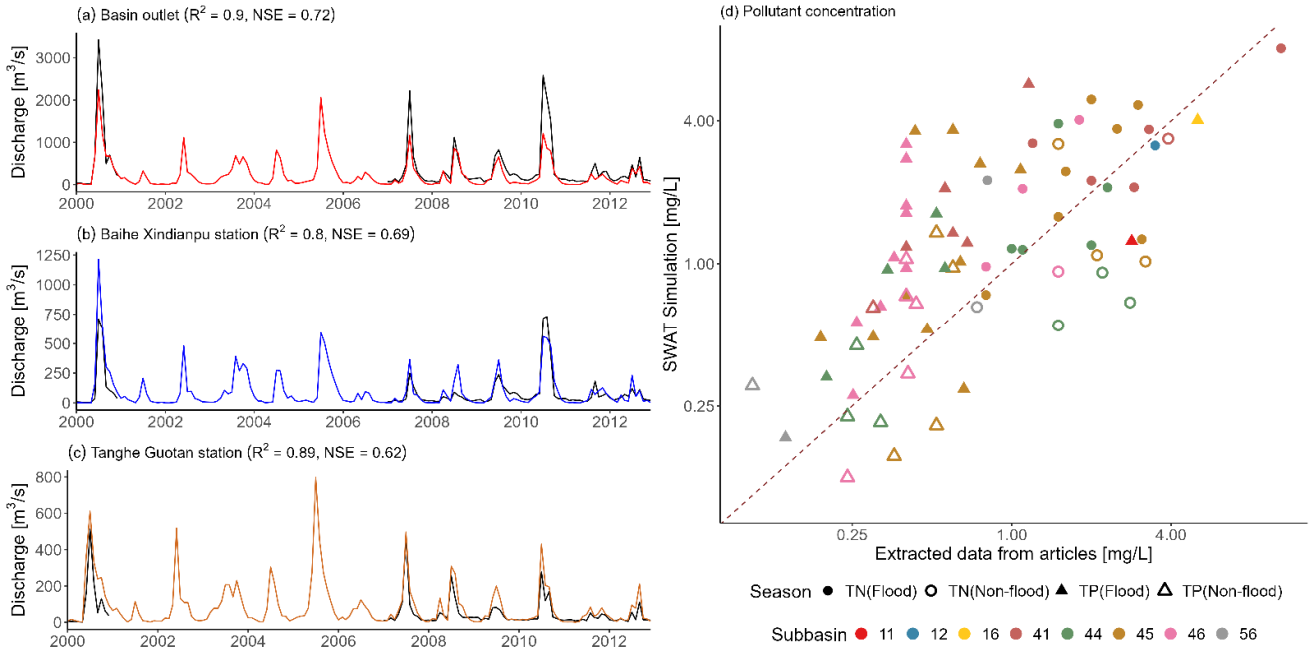

Figure 3. Comparison between SWAT simulation and record extracted from articles with respect to monthly streamflow (**a**–**c**) and TN and TP concentrations (mg/L) (**d**). The flood season refers to the months of April to September, and the non-flood season refers to the remaining months. The distribution of the subbasin index is found in the following Figure 4.

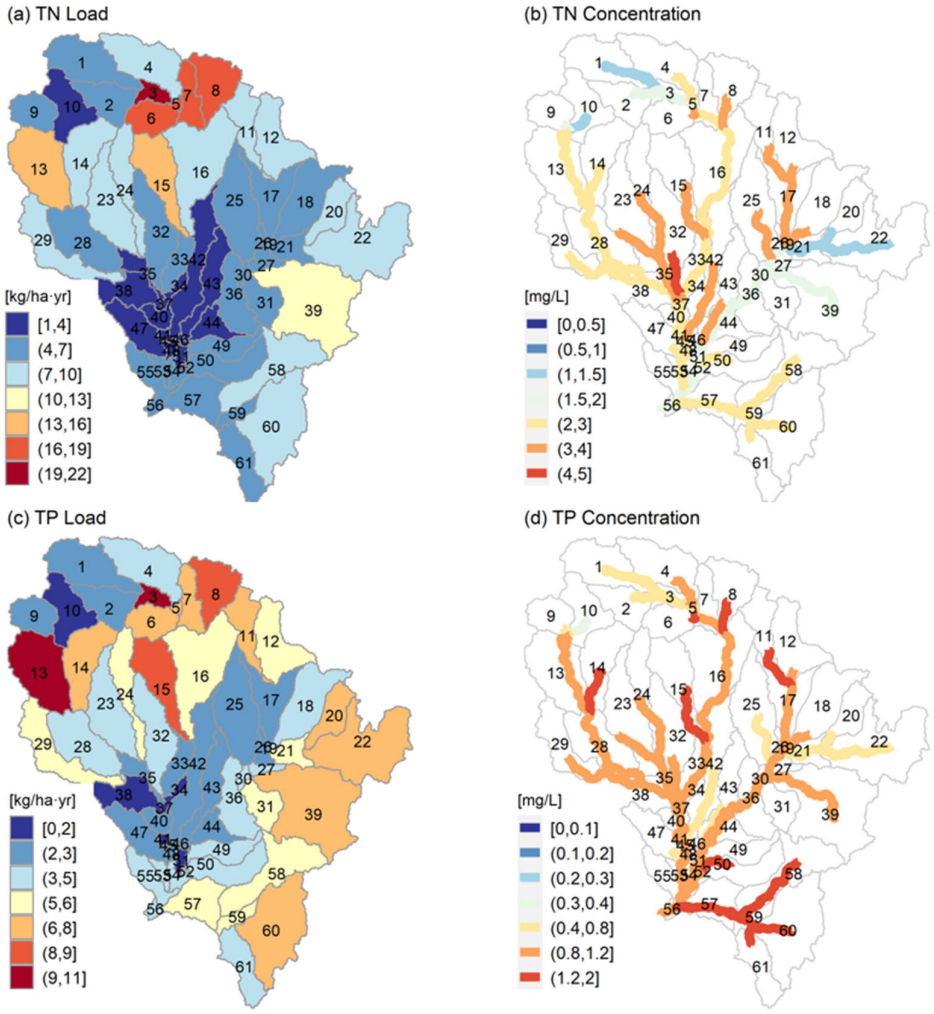

Figure 4. Spatial distribution of simulated TN (**a**,**b**) and TP (**c**,**d**) averaged over 2000–2019. Panels (**a**,**c**) are the annual mean load into reach from each subbasin and (**b**,**d**) are the mean monthly pollutant concentrations in the reach. The blue palette in (**b**,**d**) indicates concentrations of water quality of Class I (applicable to source water and national nature reserves, with TN ≤ 0.2 mg/L and TP ≤ 0.02 mg/L), Class II (primary protection zone for centralized drinking water, with TN ≤ 0.5 mg/L and TP ≤ 0.1 mg/L), Class III (secondary protection zone for centralized drinking water, with TN ≤ 1 mg/L and TP ≤ 0.2 mg/L), Class IV (undrinkable, applicable to general industrial water, with TN ≤ 1.5 mg/L and TP ≤ 0.3 mg/L), and Class V (undrinkable, applicable to agricultural water, with TN ≤ 2 mg/L and TP ≤ 0.4 mg/L), respectively, according to Environmental Quality Standards for Surface Water (GB3838-2002). The red palette indicates water quality inferior to Class V (i.e., TN > 2 mg/L and TP > 0.4 mg/L).

SWAT simulated nutrient yields are expressed as load. The term was converted from load to concentration to facilitate comparison between simulation, record, and Environmental Quality Standards for Surface Water (GB3838-2002). The total N/P load in surface water is TOT_X (X represents nitrogen or phosphorus), while that leaching from HRU or subbasin into the reach during the time step is the sum of N/P in different forms (Equations (2) and (3). The corresponding concentration C_X (mg/L) in surface water is the total load divided by the mass flow rate (Equation (4)).

$$TOT_N = ORGN + NUSRQ \quad (2)$$

$$TOT_P = ORGP + SEDP + SOLP \quad (3)$$

$$C_X = \frac{TOT_X}{FLOW_{out}} \times \eta \quad (4)$$

where TOT_N and TOT_P are total nitrogen TN (kg) and total phosphorus TP (kg) in the reach. $ORGN$ and $NUSRQ$ are organic N yield (kg N/ha) and nitrate NO_3^- transport with surface runoff into the reach (kg N/ha). $ORGP$, $SEDP$, and $SOLP$ are organic P yield (kg P/ha), mineral P in sediment transported into reach (kg P/ha), and soluble mineral forms of P transport by surface runoff (kg P/ha), respectively. $FLOW_{out}$ is the streamflow out of the reach during time step (m^3/s), and η is the unit conversion factor.

2.3. Ecological Compensation Implementation

Understanding the upstream–downstream linkage in hydrological processes and nutrient (N and P) pollution is essential. Generally, the economy of the upstream basin is relatively backwards compared to the downstream basin; thus, the conflict between economic development and water ecological protection is more pronounced. Protection of water resources in the upper regions is likely to be much more beneficial for downstream areas, especially in terms of urban landscape and ecology. For TRB, Nanyang city (in upstream Henan province) had a per capita GDP of CNY 38,064 (note: CNY 1 = USD 0.15), while Xiangyang city (in downstream Hubei province) had a GDP of 2.3 times the upstream GDP (CNY 84,815) in 2019. It is necessary to establish water pollution ecological compensation between downstream beneficiaries and upstream water protectors to achieve ecological sustainability for the entire basin.

Common river restoration measures include the collection of pollution taxes for individual polluters [38], payments for environmental services (e.g., agricultural practices) [39], conservation reserve programs [40], and conversion of cropland to forest (i.e., Grain for Green) [41]. Among them, the Grain for Green (hereinafter "GFG") measure is a widely adopted ecological restoration measure in China that is applicable to agricultural non-point-source pollution. In this study, we established four sets of GFG measures applied to AGRL lands in Henan province, thereby adjusting the economic structure and promoting industrial upgrades using funds from eco-compensation. (1) Converting all sloping drylands (AGRL, slope > 15°) in Henan province, comprising 1.5% of dryland areas in Henan, to forest (FRST); (2) converting all non-flat drylands (AGRL with slope > 2°), constituting 21.8% of drylands in Henan, to FRST; (3) converting all drylands in Henan province to FRST; and (4) performing conversions based on the AGRL area ratio (without distinguishing slopes), 10%, 20%, 40%, 60%, and 80% of the AGRL land in Henan province to FRST. For each area ratio, we generated 10 scenarios by randomly selecting HRUs of unique combinations of SOIL-LULC until the threshold area was reached. A total of 53 AGRL-to-FRST scenarios were generated, and each was used as LULC input to rerun SWAT. The corresponding nutrient (N and P) and crop yield outputs were then simulated.

The eco-compensation quantification, which is the key for implementing compensation, is always measured by monetary values. The ecosystem services were estimated based on the opportunity cost of land use. Specifically, we added up the cost of planting trees and the annual mean value of crops lost because of the GFG activities. The tree planting fees were calculated based on the annual compensation standard for state-owned forests, which is CNY 75 per hectare per year. The value of wheat was assumed to be the average purchase price in Henan in 2020, which was CNY 2.24/kg, while corn was CNY 2.62/kg. This total cost then served as the upper boundary of the compensation standard. Additionally, the lower boundary of the compensation standard was estimated according to the up-to-date national policy of the GFG program, which is subsiding CNY 4800 per hectare per year, for a total of 5 years.

3. Results and Discussion

According to the input data, the watershed is discretized into 61 subbasins and divided into 2298 HRUs. The watershed outlet (Zhangwan section on the Tangbai River–

Han River intersection) is located in subbasin 56, which drains an area of 24,200 km^2. The river sections lying at the provincial boundary, the Diwan section on the Bai River and the Bukou section on the Tang River (Figure 2d), are located in subbasins 45 and 46, with drainage areas of 11,780 km^2 and 7834 km^2, respectively.

3.1. Suitability of SWAT for Simulating Streamflow and Nutrients

SWAT model performance in simulating hydrological processes is typically determined by the fitness of the streamflow time series at the watershed outlet. According to the existing literature, when the Nash–Sutcliffe efficiency (NSE) exceeds 0.5 and the coefficient of determination (R^2) exceeds 0.6, the simulation results are deemed satisfactory [42]. Before calibration, the NSE and R^2 values for monthly streamflow at the outlet of TRB are already 0.9 and 0.72, respectively (Figure 3a). The streamflow in high-flow seasons is underestimated at the outlet. This could be related to the interpolation and aggregation of daily rainfall. The NSEs for the reaches on the tributaries also exceed 0.6, while R^2s exceed 0.8 (Figure 3b,c). According to the statistical indicators, it appears that the SWAT model has satisfactory applicability to TRB. This may be partly due to the relatively uniform distribution of meteorological inputs (Figure 2d). In contrast, simulated streamflow does not improve much after 2000 auto-calibrations using SWATCUP, a phenomenon which was also observed in another Yangtze River subbasin study [43]. Therefore, the rest of this study used the default parameters and settings, instead of the calibrated parameters. Literature discussions are available for the SWAT model calibration method, sensitivity analysis, and the possible range of parameters [44,45].

Water quality comparison in terms of concentrations of TN and TP is shown in Figure 3d. Because only a monthly step was adopted when running SWAT, the impact of daily step storm scour on nutrients cannot be considered; thus, the hydrologic condition when water was sampled (i.e., water quality data obtained from the literature) may differ from that we simulated. Most TN concentrations are greater than 1.0 mg/L and the overestimation of the SWAT model usually occurs during the flood season (April to September). TP concentrations are mostly within 1.0 mg/L but overestimation of TP is more pervasive. These frequent overestimations of N and P may likely be the result of uncalibrated parameters impacting sediment and nutrient transportation simulations. Nevertheless, we failed to calibrate the simulations as calibration requires observations of nutrient loads (kg), whereas the collected measurements are in the form of concentration (kg/L) and, more importantly, include both point and non-point sources of pollution at distinct locations. Due to the difficulty of collecting point-source pollution data, the nutrient emissions caused by industrial waste and residential sewage were not considered in this study.

In general, despite the dispersion of nutrient concentrations, the estimated values mostly fall within acceptable ranges according to available data for the study area. We claim that the SWAT model can essentially convey the hydrological processes and nutrient pollution in TRB.

3.2. Spatial and Temporal Distribution of Nutrient Pollution

3.2.1. Spatial Variation in Nutrients

As an important component in water pollution, SWAT simulates the transformation and transportation processes of N and P nutrients. Figure 4 shows the simulated spatial distribution of nutrient (TN and TP) leaching loads from each subbasin and the concentration in each river reach. The nutrients in Figure 4a,c are illustrated in terms of load per unit area (kg/ha) to make the value comparable among different subbasins with distinct total areas. The spatial distribution of non-point-source pollution strongly depends on the heterogeneities of soil properties, crop types, vegetation types, farming activities, etc. [46]. The TN load is mainly concentrated in the mountainous cultivated field of the upstream areas of the Bai River, such as subbasins 3 (22 kg/ha·y), 5–8, whereas TN load to the Tang River is lower, ranging from 2.9 kg/ha·y (subbasin 44) to 11.8 kg/ha·month (subbasin 39).

The intensity of TP load is about half that of TN load. Again, subbasin 3 leached the most TP into the river, at a rate of 10 kg/ha per year. In addition to the upper Bai River regions, TP load is also high in the southeast TRB, including the upper Tang River regions and the other tributary of the Tangbai River, the Gun River in Hubei Province. In the middle flat land, only small amounts of N and P loads are observed. This may be attributed to (1) the low altitude and (2) the occupation of shajiang black soil (Figure 2b), which belongs to a clayey soil (40–54% of clay among four layers), thereby retaining nutrients much longer and eroding less [47].

The mean monthly TN and TP concentrations at the watershed outlet are 1.9 mg/L and 1.1 mg/L, respectively. Regarding the variation along river reaches (Figure 4b,d), none have mean TN or TP concentration that met the Class III standard (i.e., ≤1.0 mg/L for TN and ≤0.2 mg/L for TP). Only 441 km (30.5%) of the river total length had TN concentrations belonging to Classes IV–V. The Bai River is more polluted with N than the Tang River. Except for reaches flowing through the northern mountainous forests, all reaches of the Bai River have TN concentrations inferior to Class V (Figure 4b). The Tang River, in contrast to the Bai River, has TN concentration in the mainstem within Class V and is only inferior to Class V in three tributaries. The magnitude of TP concentration on average is lower than that of TN, but its quality class is significantly worse. Only 18 km of river reaches are of Classes I–V. The remaining 98.8% of the rivers have TP concentrations that are inferior to Class V (Figure 4d).

Table 3 lists the nutrient inputs through fertilization and leaching for different land covers. The average N application for the whole TRB is estimated to be 114.3 kg/ha·y. The highest N fertilization occurs in hay land (HAY), where auto-fertilization is applied based on nitrogen stress and heat units (Section 2.2.2). The elemental N and P fertilizers applied to generic dryland (AGRL) are large because of chemical fertilizer application, as shown in Table 2. The three land covers with the highest TN leaching per unit area are barren land (BARR), dryland AGRL, and pasture (PAST), corresponding to 14, 10, and 9.7 kg/ha·y, respectively. The highest TP leaching is observed in agricultural fields with values of 8.4 and 7.1 kg/ha·y for RICE and AGRL, respectively. The nutrient loads from fields are dominated by organic N (ORGN in Equation 2, 92% and 86% of TN for AGRL and RICE, not shown) and sediment mineral P (SEDP in Equation 3, 68% and 77% of TP, not shown). SWAT simulates three forms of organic N/P: active organic N/P, stable organic N/P associated with humic substances, and fresh organic N/P associated with plant residues [48]. Such predominant organic N and sediment P may partly due to that (1) SWAT tends to overestimate organic N but underestimate dissolved N [49,50], and (2) the accuracy of organic N and sediment P relies on how sediment is simulated [49,51]. The SWAT model has been found to tend to overestimate organic N but underestimate dissolved N [50]. The high nutrient leaching from fields is due to the loosening surface, ponding fresh water on the soil surface, harvesting activities, and rich content of nutrients in the fields; thus, sediment and nutrients can be easily washed away or infiltrated into streams during heavy rainfall. Organic N accounts for 100% of TN losses in pasture (PAST), barren land (BARR), and forest (FRST), which is caused by rain erosion. Forests leach much less nutrients than other land covers, with 2.7 kg/ha·y for TN and 0.9 kg/ha·y for TP, owing to their complex vegetation coverage and interception effects of higher leaf area. This difference in nutrient loss is consistent with previous studies [52,53].

Table 3. The type of plant, area and area ratio, elemental nitrogen, and phosphorus fertilizers applied through calendar fertilization and auto-fertilization in HRU (Nfert, Pfert, see Section 2.2.2), and total N and total P transport from a certain HRU into reach (TN, TP) in load and load per unit area per year for individual land-use/land-cover (LULC) classes.

LULC	Plant	Area (km^2)	Area (%)	Nfert (kg/ha·y)	Pfert (kg/ha·y)	TN (kg/ha·y)	TP (kg/ha·y)	TN (ton·y)	TP (ton·y)
AGRL	WWHT/CORN	14,913.9	61.6	153.9	69.6	10.0	7.1	14,850.9	10,566.6
FRST	FRST	4462.2	18.4	-	-	2.7	0.9	1223.9	387.2
URLD	BERM	1638.0	6.8	121.2	-	5.6	1.5	917.0	252.5
RICE	RICE	1083.2	4.5	76.2	49.3	6.3	8.4	680.8	913.5
WATR	-	657.6	2.7	-	-	-	-	-	-
PAST	Panicum	567.3	2.3	-	-	9.7	3.1	550.1	173.8
HAY	Hay	392.0	1.6	321.6	12.5	3.0	1.5	118.3	60.4
URBN	BERM	221.3	0.9	226.2	-	6.6	0.3	147.1	7.5
ORCD	ORCD	142.7	0.6	2.9	-	4.1	1.1	57.9	15.0
UIDU	BERM	83.2	0.3	129.2	-	6.0	1.5	49.6	12.5
BARR	BARR	30.4	0.1	-	-	14.0	4.2	42.6	12.8
Whole basin		24,192	100	114.3	45.3	7.7	5.1	18,638.2	12,401.8

The annual mean loads of N and P leaching from HRUs to stream for the whole TRB are 18.6 and 12.4 kiloton, respectively (see Table 3), whereas the corresponding loads flowing through the watershed outlet (reach 56) are slightly lower at 16.2 (13% less) and 11.6 (6.5% less) kiloton (see Figure 5). When area factions of different land covers are considered, AGRL land is the predominant source of nutrient pollution in the Tangbai River, constituting 79.7% of TN and 85.2% of TP. Such serious non-point-source pollution should be controlled by strengthening dryland management and emphasizing conservation tillage to reduce sediment and nutrient losses.

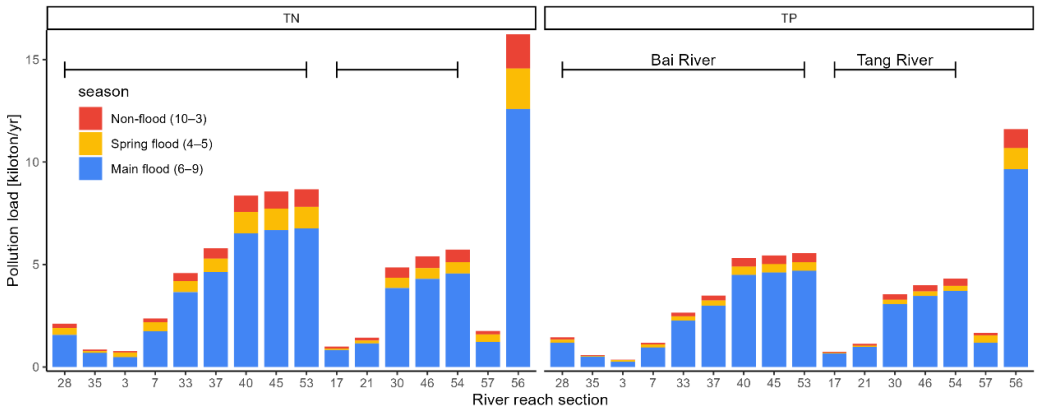

Figure 5. Seasonal mean TN and TP loads transported with water out of the individual river reaches averaged over 2000–2019. Reaches numbered before 53 belong to the Bai River, and those numbered 17–54 belong to the Tang River. Reach 57 is the downstream tributary called the Gun River, and 56 is the watershed outlet of TRB.

3.2.2. Seasonal Variation in Nutrients

We divided the year into three seasons according to the monthly variation in precipitation: the non-flood season (from October to March), spring flood season (April and May), and main flood season (June to September). The respective mean seasonal total precipitation from 2000–2019 are 174.9 mm (21% of the mean annual), 150.6 mm (18%), and 497.4 mm (61%). Figure 5 shows the TN and TP loads at each representative reach for the three seasons. The nutrient loads are overwhelmingly dominant in the main flood season,

constituting on average 78% of the annual TN load and 84% of the TP load. Using the watershed outlet (reach 56) as an example, the TN loads in spring flood season and main flood season are approximately 3.5 and 9 times that in the non-flood season, respectively; the TP loads are 3.3 and 16 times that in the non-flood season, respectively. The simulated low nutrient pollution in non-flood seasons is because the pollutants gradually accumulate on the land surface when there is little or no rain, regardless of the point-source pollution emissions. The spring flood season is the first period of concentrated rainfall after the dry winter; thus, it allows the pollutants accumulated in the soil and floating in the air to be washed away into the stream.

Comparing the loads of different reaches, a clear increasing trend of nutrients is observed from upstream to downstream, suggesting relatively lower rate of pollutant degradation than accumulation. For example, except for the two reaches 28 and 35, which are tributaries of the Bai River (Figure 4b), TN and TP loads increase continuously along reaches 3 to 53. The changes among reaches 40, 45, and 53 are limited because the leaching losses from the respective subbasins are low (Figure 4a,c). The TN load in the Bai River (reach 53) is around 1.5 times that of the Tang River (reach 54), accounting for around 53.4% and 35.3% of total nutrient loads at the outlet reach 56. The TP loads in the Tang River and the lower reaches of the Tangbai River contribute more to that in reach 56, as a result of increasing phosphorus loss from paddy fields (RICE, Table 3) which are distributed mainly in the southern part of TRB (Figure 2a).

3.2.3. Nutrients in the Trans-Provincial Key Sections

The trans-provincial analysis focuses on three controlled sections, including the outlet of TRB (Zhangwan section on reach 56) and the junctions of Henan and Hubei province (Diwan section and Bukou section on reaches 45 and 46). Figure 6 illustrates the monthly distribution of nutrient concentrations in these sections. Both the multi-year mean and median results are shown to eliminate the disturbance from large outliers.

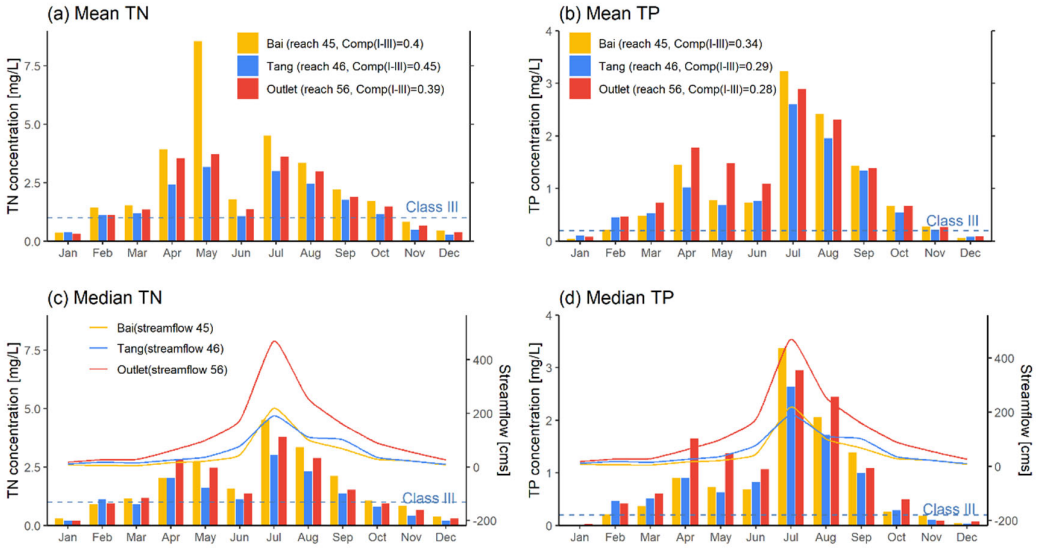

Figure 6. Mean and median values of monthly TN (**a**,**c**) and TP (**b**,**d**) concentrations in reaches 45 (Diwan section) on the Bai River, 46 (Bukou section) on the Tang River, and 56 (Zhangwan section) of the watershed outlet. The dashed horizontal lines are the respective concentrations of water quality Class III. The three curves in (**c**,**d**) are SWAT-simulated mean monthly streamflow for the individual reaches. Comp(I–III) in the legend is the respective compliance rate of Classes I–III water in the period 2000–2019.

Nutrient pollution is concentrated during the flood season (April to September): it increases sharply in April, decreases in June, peaks in July, and then gradually declines with decreasing streamflow. In accordance with Figure 5, the nutrient concentration is high in the spring flood season (April and May) despite the small proportion of annual rainfall and streamflow. The N and P leaching losses under heavy rainfall during the spring flood season far exceed those under weak rainfall during the non-flood season, which is consistent with previous findings [54]. This in turn causes the nutrient concentration to exceed the water quality standard. For the Bai River, the mean TN concentration in the spring flood season can be even higher than that in the main flood season. Interestingly, we find the mean TN (Figure 6a) to be much larger than the median value (Figure 6c), while the difference is insignificant in the remaining months. This indicates that the extremely high TN concentration on the Bai River can occur during spring flood seasons. In contrast, the TP concentration in the spring flood season is only about half of the peak value (in July). This is because paddy fields (RICE), which are the main source of P pollutants (Table 3), lay fallow in the non-flood season (Table 2); therefore, phosphorus accumulation is limited in winter, and the amount of P flushed out from paddy fields is also not high during the spring flood season.

Considering the water quality standard, the Class III water quality compliance rate for monthly TN concentration over 2000–2019 is around 40%, and for TP, it is only 30%. The higher compliance rate of TN than TP is consistent with the spatial distribution results in Figure 4. On average, only months in the non-flood season (October to March) may reach Class III or Class V water. The TN pollution in the Bai River is more serious than that in the Tang River; but the opposite is true for TN pollution.

3.3. Effect and Quantification of Eco-Compensation

Stretching across Henan province (Nanyang city) and Hubei province (Xiangyang city), TRB has a high proportion of traditional agriculture. Nanyang has 86.8% of the total agricultural fields of TRB, while Xiangyang has only 13.2%. The boundary between wheat–corn fields and rice fields almost coincides with the provincial boundary between Henan and Hubei provinces. Nanyang city has been accustomed to growing wheat and corn for thousands of years for geographical reasons. The major soil types in Nanyang are shajiang black soil (SJHT) and yellow-cinnamon soil (HHT, Figure 2b). Both are typical low-yield soils due to their low organic matter content and poor soil structure [55,56]. The wide extent of dryland farming in Henan province, along with intensive human activities, has accelerated soil erosion, leading to serious nutrient losses.

To realize the simultaneous growth of the economy and restoration of water ecosystems in Nanyang city, increasing crop yield, for example, through implementing more scientific crop management (e.g., agricultural industrial agglomeration) and a higher portion of organic fertilizer [57], is necessary but not sufficient. It is an inevitable trend to abandon part of drylands, and transform and upgrade the local industrial structure. This section predicts the effect of converting dryland to forest on water quality in streams across the provincial boundary. Note that we assume that dryland fields (AGRL) in Hubei province and all paddy fields (RICE) remain unchanged because (1) this study investigates trans-boundary eco-compensation, the logic of which is the downstream Hubei province may benefit from the ecological contribution of Nanyang in the upstream and, in turn, compensate for this contribution; (2) the soil type in the paddy fields is mostly paddy soil (SDT), which is one of the three high-yield soils in China; thus the ecological benefits of retiring paddy fields are likely to be much fewer than the economic benefits of retaining farming.

Figure 7 shows the changes in pollutants and reference eco-compensation values at trans-provincial sections under different 53 Grain for Green (GFG) settings (see Section 2.3). Overall, a clearly more noticeable nutrient load decrease is observed compared to the TN/TP compliance rate increase with the increase in GFG area. For instance, up to 60% area achieves only limited improvement (within 10%) for the TP compliance rate while

the TP load is reduced by more than 50% (Figure 7b,d). Under the same horizontal axis, there is a disparity in results because the HRUs for GFG are randomly selected, either in the upper regions of the Tang River or Bai River. However, for the whole basin, the different selections in HRUs bring only limited difference in the nutrient pollution (i.e., thin ribbons for the basin outlet shown in Figure 7e). If all dryland fields in TRB in Henan province could be converted to forest (i.e., 100% GFG area), the water compliance rate in the Diwan and Bukou sections would increase by 32%–39%. The months with the worst water quality are mainly concentrated in Spring (March to May, Figure 8e,f). However, the improvement in TN at the outlet section is stronger than that in TP, with maximum increases in the compliance rate in TN of 29.8% and in TP of only 13.2%. Under the 100% GFG, the further accumulation of TN and TP loads in the downstream Hubei province is responsible for 38% and 62% of the N and P transported out of the basin, respectively. This implies that TP pollution is more extensive in Hubei and therefore cannot be controlled by eco-protection measures in Henan province only.

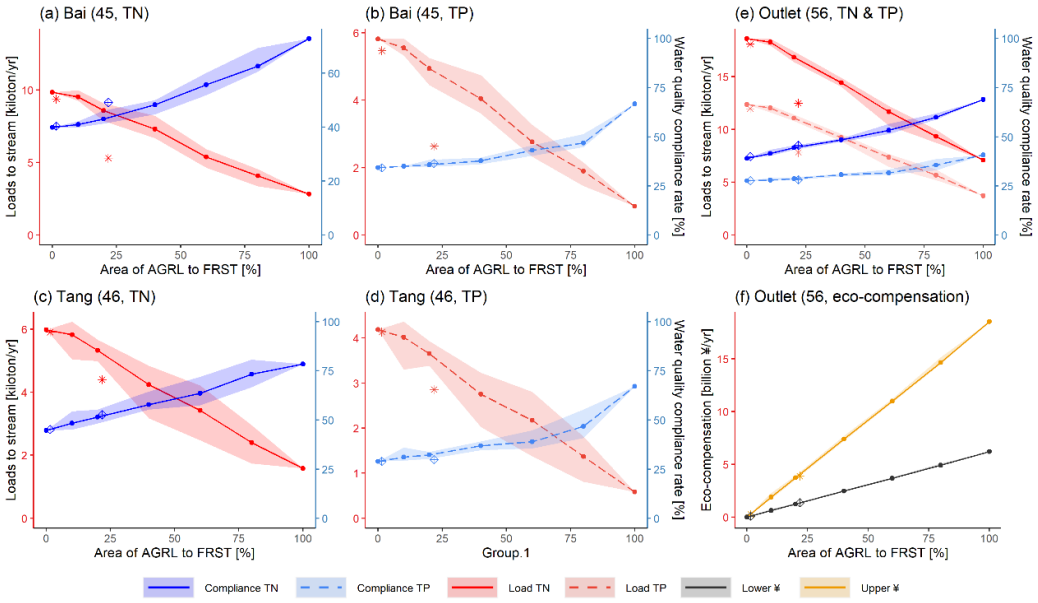

Figure 7. Effects of converting drylands (AGRL) in Henan to forest in terms of TN and TP leaching into reaches from upstream subbasins and compliance rate of water quality (Class III water) in the individual controlled sections (**a**–**e**), and the value of eco-compensations in CNY based on opportunity cost (upper line, **f**) and GFG compensation standard (lower line, **f**). The ribbons are the range and means of the respective results for GFG based on certain area ratios, and the scatter diamonds and stars are results based on slopes.

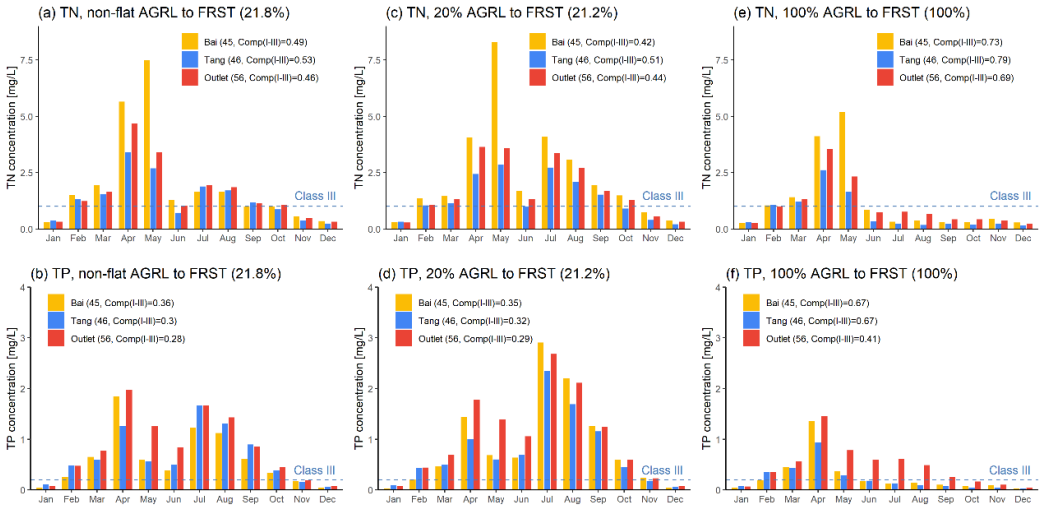

Figure 8. Comparison of mean monthly TN (**a**,**c**,**e**) and TP (**b**,**d**,**f**) concentrations in pollutant control sections between three different sets of GFG scenarios: converting all non-flat drylands (AGRL with slope > 2.5%) in Henan province to FRST (**a**,**b**), one scenario of randomly selecting 20% AGRL to FRST based on HRUs (**c**,**d**), and converting all AGRL land to FRST (**e**,**f**).

As sloping lands are more susceptible to soil erosion, the scatter dots in Figure 7 depict the two slope-specific GFG scenarios. It is evident that GFG of sloping drylands (slope > 15°, area = 1.5%) and non-flat drylands (slope > 2°, area = 21.8%) are more effective in controlling nutrient loss than slope-independent GFG scenarios. Using the TN load at the Diwan section (on the Bai River, Figure 7a) as an example, the TN reduction under the 21.8% non-flat dryland GFG is 3.5 times the mean reduction under the 20% slope-independent GFG; however, water quality compliance rates in this section are not much different from each other. This inconsistency is because although GFG of sloping/non-flat drylands reduces the pollutant load considerably, mainly in the main flood season (June to September), TN or TP concentrations during this period are still worse than Class III (Figures 8a,b and 6a,b).

To summarize, if the water quality standard is the only benchmark, then improving the nutrient concentration at the provincial boundary sections requires control of both the amount of nutrients being washed out and the timing of their washing out. Thus, enhancing the monitoring and management of water quality, along with the ecological operation of water projects, are the key engineering measures that allow water bodies to self-purify more effectively.

The payments of eco-compensation are calculated based on the GFG area and crop yields (Figure 7f). In the baseline scenario without any GFG, the mean annual yields of maize and wheat in TRB within Henan province are 3839.1 and 3740.7 kiloton, respectively. The sum of this is close to, but slightly higher than, the statistic annual grain production of 7105.9 kiloton in Nanyang city in 2019 [58]. The total average annual value of both crops simulated by SWAT is CNY 18.4 billion. The compensation amount considering agricultural opportunity costs increases almost linearly with the increase in GFG area, from CNY 1.81 billion (for 10% GFG) to CNY 18.4 billion (for 100% GFG) (upper line in Figure 7f) per year. When compensation is based on merely the GFG area, the value also increases proportionally, but grows more slowly (lower line in Figure 7f). Under the 100% GFG scenario, the lower value is only one-third of the upper value. This indicates that even under the same ecological restoration strategy, the amount of eco-compensation available to farmers may vary considerably due to the different quantitative criteria adopted.

3.4. Implications for Eco-Compensation

In China, the main factors accounting for eco-compensation include the following three with reference to guidelines in other countries. (1) The opportunity-cost factor: additional consideration must be given to opportunity costs, which are the non-ecological benefits being sacrificed by environmental protectors to protect the environment [59]. (2) The polluter-pays factor: the actors causing the pollution should pay to correct the wrong, thereby limiting their pollution activities and effectively reducing the environmental free-riding behaviors [60]. (3) The beneficiary-pays factor: beneficiaries of ecosystem services should reimburse the upstream providers of water-related environmental services either in full or according to a share of the total [61,62]. Generally, the finance of eco-compensation in China comes from both the government and directly responsible stakeholders [41]. The calculations performed in this study, especially Figure 7f, can provide the bases for estimating opportunity cost. Although the money involved may seem large, it does not reflect the actual amount of funds needed for reforestation but provides reference boundaries of the investment that needs to be paid to the upstream by downstream water users. Local ecological requirements and financial affordability should be considered when accounting for eco-compensation and making decisions.

Funding for watershed protection can be implemented in two ways. The first is paying for ecological projects, such as water project construction, including sewage treatment and ecological restoration plants, and their subsequent maintenance. The second is to directly subsidize the contributors of the affected areas, such as paying out the protection funds to the residents, enterprises, and local governments involved on an annual or quarterly basis to compensate their losses due to changes in crop production and lifestyles. The former project payment can promote regional sustainable development and maintain long-term operation, but fixed, static investments may lack flexibility [63]. In contrast, the latter subsidy, although highly flexible and easily gains trust from local residents, can easily turn into consumption expenditure [64], thereby deviating from the policy objective of agricultural transformation. In this study area, the eco-compensation fund needs to be allocated in a combination of project support and subsidies. That is, to achieve a good water ecosystem status in the downstream TRB, it is necessary not only to carry out integrated management at the watershed level but also to provide cash payments to the upstream government and residents, especially to farmers who return farmland to forest.

The standards of eco-compensation can be determined through negotiation based on project cost analysis and water value assessment [65] or on flexible gambling agreements [66]. The value assessment can be calculated by incorporating both direct cost and opportunity cost, such as the money inputs for pollutant dilution and the lost development opportunities due to ecological protection activities. The gambling agreement is more often utilized for eco-compensation regarding trans-regional water protection, where negotiation is made between upstream and downstream in terms of water quality standards and pollutant thresholds in the controlled river sections. If the water quality at the junctions meets the standards, the co-protection fund should be allocated upstream as compensation for protecting the watershed; conversely, the fund will be given downstream as compensation for purifying water.

4. Conclusions

The Tangbai River Basin (TRB) is a typical trans-provincial watershed in central China that experiences severe non-point-source agricultural pollution. Based on the SWAT model simulations in TRB, the spatial and temporal distributions of nitrogen and phosphorus pollution are described in terms of nutrient load and concentration. Their responses to Grain for Green (GFG) ecological restoration measures are then investigated. With respect to trans-regional eco-compensation, we evaluated the effects of location, area, and the slope-dependency of GFG on the water quality along the provincial boundary sections, using TN and TP as indicators. It appears that GFG measures may be more

effective at reducing nutrient loads than increasing the water quality compliance rate. The monetary values of the corresponding eco-compensation are quantified based on crop production changes and the GFG area. We found that the compensation amount using opportunity cost can be as high as three times the amount typically paid based on area. This study could provide suggestions for eco-compensation and offer new ideas for controlling non-point-source pollution of trans-boundary rivers.

Author Contributions: W.W., H.Z. and Y.L. planned the study and prepared the initial data. W.W. performed computations and data analysis and wrote the initial draft. H.Z. supervised the writing of the paper. Y.F. coordinated a part of computation. H.Z. and H.F. provided financial support. The revised version was written by W.W., with specific contribution from H.Z. and J.Z. All authors have read and agreed to the published version of the manuscript.

Funding: This research was supported by the National Natural Science Foundation of China, (No. 52179009, 51909035 and U2040206).

Institutional Review Board Statement: Not applicable.

Informed Consent Statement: Not applicable.

Data Availability Statement: The public datasets used for SWAT model building have been properly cited in the main text, while the data of streamflow and nutrient concentration adopted for model validation can be found in https://doi.org/10.6084/m9.figshare.20402019.

Conflicts of Interest: The authors declare that they have no known competing financial interests or personal relationships that could have appeared to influence the work reported in this paper.

References

1. Prathumratana, L.; Sthiannopkao, S.; Kim, K.W. The relationship of climatic and hydrological parameters to surface water quality in the lower Mekong River. *Environ. Int.* **2008**, *34*, 860–866.
2. Zeitoun, M.; Goulden, M.; Tickner, D. Current and future challenges facing transboundary river basin management. *WIREs Clim. Chang.* **2013**, *4*, 331–349.
3. Connell, D.; Grafton, R.Q. Water reform in the Murray-Darling Basin. *Water Resour. Res.* **2011**, *47*, W00G03.
4. Isakson, R.S. *Payments for Environmental Services in the Catskills: A Socio-Economic Analysis of the Agricultural Strategy in New York City's Watershed Management Plan*; Report was Elaborated for the "Payment for Environmental Services in the Americas" Project, FORD Foundation and Fundación PRISMA: San Salvador, El Salvador, 2002.
5. Ren, Y.; Lu, L.; Yu, H.; Zhu, D. Game strategies in government-led eco-compensation in the Xin'an River Basin from the perspective of the politics of scale. *J. Geogr. Sci.* **2021**, *31*, 1205–1221.
6. Jiang, K.; Merrill, R.; You, D.; Pan, P.; Li, Z. Optimal control for transboundary pollution under ecological compensation: A stochastic differential game approach. *J. Clean. Prod.* **2019**, *241*, 118391.
7. Pagiola, S.; Platais, G. *Payments for Environmental Services*; World Bank: Washington, DC, USA, 2002.
8. Adhikari, B. *Market-Based Approaches to Environmental Management: A Review of Lessons from Payment for Environmental Services in Asia*; Asian Development Bank Institute: Tokyo, Japan, 2009.
9. Sun, X.Z.; Xie, G.D.; Zhen, L. Effects of converting arable land into forest (grassland) and eco-compensation: A case study in Yuanzhou county, Guyuan city of Ningxia Hui Autonomous Region. *Resour. Sci.* **2007**, *29*, 194–200. (In Chinese)
10. Xian, J.; Xia, C.; Cao, S. Cost–benefit analysis for China's Grain for Green Program. *Ecol. Eng.* **2020**, *151*, 105850.
11. Wang, J.; Tian, R.; Dong, Z.; Shi, G.; Hou, C. *Watershed Eco-Compensation in China: Practice and Review*; Springer: Singapore, 2022; pp. 1–37.
12. Wang, H.; Dong, Z.; Xu, Y.; Ge, C. Eco-compensation for watershed services in China. *Water Int.* **2016**, *41*, 271–289.
13. Chen, C.; Matzdorf, B.; Zhen, L.; Schroeter, B. Social-Network Analysis of local governance models for China's eco-compensation program. *Ecosyst. Serv.* **2020**, *45*, 101191.
14. Reckhow, K.H.; Norris, P.E.; Budell, R.J.; Di Toro, D.M.; Galloway, J.N.; Greening, H.; Sharpley, A.N.; Shirmohammadi, A.; Stacey, P.E. *Achieving Nutrient and Sediment Reduction Goals in the Chesapeake Bay: An Evaluation of Program Strategies and Implementation*; National Academies Press: Washington, DC, USA, 2011.
15. Tang, W.; Pei, Y.; Zheng, H.; Zhao, Y.; Shu, L.; Zhang, H. Twenty years of China's water pollution control: Experiences and challenges. *Chemosphere* **2022**, *295*, 133875.
16. Jin, X.; Xu, Q.; Huang, C. Current status and future tendency of lake eutrophication in China. *Sci. China Ser. C Life Sci.* **2005**, *48*, 948–954.
17. Wu, Z.; Zhang, D.; Cai, Y.; Wang, X.; Zhang, L.; Chen, Y. Water quality assessment based on the water quality index method in Lake Poyang: The largest freshwater lake in China. *Sci. Rep.* **2017**, *7*, 17999.

18. Boesch, D.F.; Brinsfield, R.B.; Magnien, R.E. Chesapeake Bay eutrophication: Scientific understanding, ecosystem restoration, and challenges for agriculture. *J. Environ. Qual.* **2001**, *30*, 303–320.
19. Singh, A.; Imtiyaz, M.; Isaac, R.K.; Denis, D.M. Comparison of soil and water assessment tool (SWAT) and multilayer perceptron (MLP) artificial neural network for predicting sediment yield in the Nagwa agricultural watershed in Jharkhand, India. *Agric. Water Manag.* **2012**, *104*, 113–120.
20. Li, Z.; Luo, C.; Xi, Q.; Li, H.; Pan, J.; Zhou, Q.; Xiong, Z. Assessment of the AnnAGNPS model in simulating runoff and nutrients in a typical small watershed in the Taihu Lake basin, China. *Catena* **2015**, *133*, 349–361.
21. Redhead, J.W.; May, L.; Oliver, T.H.; Hamel, P.; Sharp, R.; Bullock, J.M. National scale evaluation of the InVEST nutrient retention model in the United Kingdom. *Sci. Total Environ.* **2018**, *610*, 666–677.
22. Arnold, J.G.; Moriasi, D.N.; Gassman, P.W.; Abbaspour, K.C.; White, M.J.; Srinivasan, R.; Santhi, C.; Harmel, R.D.; Van Griensven, A.; Van Liew, M.W. SWAT: Model use, calibration, and validation. *Trans. ASABE* **2012**, *55*, 1491–1508.
23. Sharp, R.; Tallis, H.T.; Ricketts, T.; Guerry, A.D.; Wood, S.A.; Chaplin-Kramer, R.; Nelson, E.; Ennaanay, D.; Wolny, S.; Olwero, N. *InVEST User's Guide*; The Natural Capital Project: Stanford, CA, USA, 2014.
24. Bingner, R.L.; Theurer, F.D. AGNPS 98: A Suite of Water Quality Models for Watershed Use. In Proceedings of the Federal Inter-Agency Sedimentation Conference 7, Reno, NV, USA, 25–29 March 2001; pp. 1–8.
25. Hoang, L.; van Griensven, A.; Mynett, A. Enhancing the SWAT model for simulating denitrification in riparian zones at the river basin scale. *Environ. Modell. Softw.* **2017**, *93*, 163–179.
26. Shrestha, S.; Bhatta, B.; Shrestha, M.; Shrestha, P.K. Integrated assessment of the climate and landuse change impact on hydrology and water quality in the Songkhram River Basin, Thailand. *Sci. Total Environ.* **2018**, *643*, 1610–1622.
27. Huang, Q.; Huang, Q. Tangbai River Water Pollution and Prevention Measures. *Yangtze River* **1999**, *30*, 30. (In Chinese)
28. STHJT. Monthly Report on Water Quality of Han River. Available online: http://sthjj.xiangyang.gov.cn/hjxx/tjsj/hjszyb/ (accessed on 1 May 2021). (In Chinese)
29. Yao, C. Pollution of Tangbai River Basin Endangers Hubei and Henan Provinces. Available online: http://www.xfmj.gov.cn/cms/html/jianyanxiance/20100304/65.html (accessed on 1 February 2021). (In Chinese)
30. State Council; Ministry of Natural Resources; National Bureau of Statistics. *Technical Regulations of the Third National Land Survey*; State Council; Ministry of Natural Resources; National Bureau of Statistics: Beijing, China, 2018 (In Chinese)
31. Cai, X.; Xu, Z.; Su, B.; Yu, W. Distributed simulation for regional evapotranspiration and verification by using remote sensing. *Trans. CSAE* **2009**, *25*, 154–160. (In Chinese)
32. Cai, L. Investigation on Agricultural Non-point Source Pollution in Henan Province. Master's Thesis, Henan University, Kaifeng, China, 2017. (In Chinese)
33. Lan, S. Investigation and Research on Agricultural Non-point Source Pollution in Nanyang City. *Agro-Environ. Dev.* **2009**, *26*, 59–61. (In Chinese)
34. Nanyang Agricultural Bureau. Guiding Opinions on Scientific Fertilization of Crops in Nanyang City in 2019. Available online: http://nyj.nanyang.gov.cn/ (accessed on 1 May 2021). (In Chinese)
35. Shi, J.; Zhou, S.; Zhao, J.; Dong, B. Livestock and Poultry Manure Excrements and Their Environmental Effect Evaluation in Nanyang. *J. Domest. Anim. Ecol.* **2014**, *35*, 76–81. (In Chinese)
36. Liu, X.; Kuang, M.; Dai, Z.; Wang, M.; Xie, B. Water pollution analysis and control measures of Tangbai river. *J. Chongqing Univ. Arts Sci.* **2014**, *33*, 5. (In Chinese)
37. Zhang, S.; Lin, L.; Wang, Z.; Pan, X.; Liu, M.; Dong, L.; Tao, J. Spatio-temporal Variation of Water Quality in the Middle-lower Hanjiang River. *J. Yangtze River Sci. Res. Inst.* **2020**, *38*, 7. (In Chinese)
38. Hass, J.E. Optimal taxing for the abatement of water pollution. *Water Resour. Res.* **1970**, *6*, 353–365.
39. Branca, G.; Lipper, L.; Neves, B.; Lopa, D.; Mwanyoka, I. Payments for watershed services supporting sustainable agricultural development in Tanzania. *J. Environ. Dev.* **2011**, *20*, 278–302.
40. Dunn, C.P.; Stearns, F.; Guntenspergen, G.R.; Sharpe, D.M. Ecological benefits of the conservation reserve program. *Conserv. Biol.* **1993**, *7*, 132–139.
41. Delang, C.O.; Yuan, Z. *China's Grain for Green Program*; Springer: Cham, Switzerland, 2016.
42. Moriasi, D.N.; Gitau, M.W.; Pai, N.; Daggupati, P. Hydrologic and Water Quality Models: Performance Measures and Evaluation Criteria. *Trans. ASABE* **2015**, *58*, 1763–1785. https://doi.org/10.13031/trans.58.10715.
43. Liu, R.; Xu, F.; Zhang, P.; Yu, W.; Men, C. Identifying non-point source critical source areas based on multi-factors at a basin scale with SWAT. *J. Hydrol.* **2016**, *533*, 379–388.
44. Hoang, L.; Van Griensven, A.; van der Keur, P.; Refsgaard, J.C.; Troldborg, L.; Nilsson, B.; Mynett, A. Comparison and Evaluation of Model Structures for the Simulation of Pollution Fluxes in a Tile-Drained River Basin. *J. Environ. Qual.* **2014**, *43*, 86–99.
45. Karki, R.; Srivastava, P.; Bosch, D.D.; Kalin, L.; Lamba, J.; Strickland, T.C. Multi-Variable Sensitivity Analysis, Calibration, and Validation of a Field-Scale SWAT Model: Building Stakeholder Trust in Hydrologic and Water Quality Modeling. *Trans. ASABE* **2020**, *63*, 523–539.
46. Helfand, G.E.; House, B.W. Regulating nonpoint source pollution under heterogeneous conditions. *Am. J. Agric. Econ.* **1995**, *77*, 1024–1032.
47. Richardson, C.W.; King, K.W. Erosion and nutrient losses from zero tillage on a clay soil. *J. Agric. Eng. Res.* **1995**, *61*, 81–86.
48. Neitsch, S.L.; Arnold, J.G.; Kiniry, J.R.; Williams, J.R. *Soil and Water Assessment Tool Theoretical Documentation Version 2009*; Texas Water Resources Institute: Forney, TX, USA, 2011.

49. Van Kessel, C.; Clough, T.; van Groenigen, J.W. Dissolved organic nitrogen: An overlooked pathway of nitrogen loss from agricultural systems? *J. Environ. Qual.* **2009**, *38*, 393–401.
50. Yuan, Y.; Chiang, L. Sensitivity analysis of SWAT nitrogen simulations with and without in-stream processes. *Arch. Agron. Soil Sci.* **2015**, *61*, 969–987.
51. Chaubey, I.; Migliaccio, K.W.; Green, C.H.; Arnold, J.G.; Srinivasan, R. Phosphorus modeling in soil and water assessment tool (SWAT) model. In *Modeling Phosphorus in the Environment*; CRC Press: Boca Raton, FL, USA, 2006; pp. 163–187.
52. Davis, M. Nitrogen leaching losses from forests in New Zealand. *N. Z. J. For. Sci.* **2014**, *44*, 2.
53. Zhang, Y.; Li, P.; Liu, X.; Xiao, L.; Shi, P.; Zhao, B. Effects of farmland conversion on the stoichiometry of carbon, nitrogen, and phosphorus in soil aggregates on the Loess Plateau of China. *Geoderma* **2019**, *351*, 188–196.
54. Huo, D.; Gan, N.; Geng, R.; Cao, Q.; Song, L.; Yu, G.; Li, R. Cyanobacterial blooms in China: Diversity, distribution, and cyanotoxins. *Harmful Algae* **2021**, *109*, 102106.
55. Malik, Z.; Malik, M.A.; Zong, Y.; Lu, S. Physical properties of unproductive soils of Northern China. *Int. Agrophys.* **2014**, *28*, 4.
56. Liu, X.; Zhang, D.; Li, H.; Qi, X.; Gao, Y.; Zhang, Y.; Han, Y.; Jiang, Y.; Li, H. Soil nematode community and crop productivity in response to 5-year biochar and manure addition to yellow cinnamon soil. *BMC Ecol.* **2020**, *20*, 39.
57. Wei, J.; Jin, Y.; Gao, H.; Chang, J.; Zhang, L. Effects of fertilization practices on infiltration in Shajiang black soils. *Zhongguo Shengtai Nongye Xuebao/Chin. J. Eco-Agric.* **2014**, *22*, 965–971.
58. Nanyang Municipal Bureau of Statistics. *Statistical Bulletin on National Economic and Social Development of Fujian Province in 2021*; Fujian International Investment Promotion Center: Xiamen, China, 2019.
59. Kosoy, N.; Martinez-Tuna, M.; Muradian, R.; Martinez-Alier, J. Payments for environmental services in watersheds: Insights from a comparative study of three cases in Central America. *Ecol. Econ.* **2007**, *61*, 446–455.
60. Gaines, S.E. The polluter-pays principle: From economic equity to environmental ethos. *Tex. Int'l LJ* **1991**, *26*, 463.
61. He, S.; Su, Y.; Wang, L.; Gallagher, L.; Cheng, H. Taking an ecosystem services approach for a new national park system in China. *Resour. Conserv. Recycl.* **2018**, *137*, 136–144.
62. Shang, W.; Gong, Y.; Wang, Z.; Stewardson, M.J. Eco-compensation in China: Theory, practices and suggestions for the future. *J. Environ. Manag.* **2018**, *210*, 162–170.
63. Gersonius, B.; Ashley, R.; Pathirana, A.; Zevenbergen, C. Climate change uncertainty: Building flexibility into water and flood risk infrastructure. *Clim. Change* **2013**, *116*, 411–423.
64. Li, W.; Chen, J.; Zhang, Z. Forest quality-based assessment of the Returning Farmland to Forest Program at the community level in SW China. *For. Ecol. Manag.* **2020**, *461*, 117938.
65. Wu, Z.; Guo, X.; Lv, C.; Wang, H.; Di, D. Study on the quantification method of water pollution ecological compensation standard based on emergy theory. *Ecol. Indic.* **2018**, *92*, 189–194.
66. Gu, Q.; Zhang, Y.; Ma, L.; Li, J.; Wang, K.; Zheng, K.; Zhang, X.; Sheng, L. Assessment of reservoir water quality using multivariate statistical techniques: A case study of Qiandao Lake, China. *Sustainability* **2016**, *8*, 243.